

THE GEOMETRY OF RECTANGULAR MULTISSETS

MICHAEL DOUGHERTY AND JON MCCAMMOND

ABSTRACT. This article describes a natural piecewise Euclidean bisimplicial cell structure for the space of n -element multisets in a fixed Euclidean rectangle. In particular, we highlight some connections with spaces of complex polynomials and permutahedra.

INTRODUCTION

For each topological space X and positive integer n , the symmetric group SYM_n acts on the n -fold product X^n by permuting coordinates, and the quotient by this action is the *multiset space* $\text{MULT}_n(X)$.

If \mathbf{I} is isometric to a compact interval in \mathbb{R} , then the space \mathbf{I}^n is an n -dimensional cube and $\text{MULT}_n(\mathbf{I})$ is a metric simplex known as a standard n -dimensional orthoscheme. The face poset of $\text{MULT}_n(\mathbf{I})$ is the poset of *linear compositions of n* , which is denoted $\text{COMP}_n(\longleftrightarrow)$ and is isomorphic to the Boolean lattice with its minimum element removed.

In this article, we are interested in the multiset space $\text{MULT}_n(\mathbf{Q})$, where \mathbf{Q} is isometric to a closed rectangle in the complex plane. Our first result is to describe a cell structure for $\text{MULT}_n(\mathbf{Q})$, which is *bisimplicial* in the sense that every cell is a product of two simplices, as well as an analogous poset $\text{COMP}_n(\square)$ which records the incidence of faces.

Theorem A (Theorem 3.8). *Let \mathbf{Q} be a closed rectangle and let n be a positive integer. Then the multiset space $\text{MULT}_n(\mathbf{Q})$ is isometric to a bisimplicial piecewise Euclidean cell complex with face poset equal to $\text{COMP}_n(\square)$.*

For our second main theorem, we require two definitions. First, the *dual graph* of a cell complex is formed by placing a vertex in the interior of each top-dimensional cell, then connected two vertices if their corresponding cells share a face of codimension 1. Next, if S is the standard generating set of adjacent transpositions $\{\sigma_1, \dots, \sigma_{n-1}\}$ for the symmetric group SYM_n , then we define $\Gamma^{LR}(\text{SYM}_n, S)$ to be the graph obtained by overlaying the left and right Cayley graphs of SYM_n with respect to S . In other words, the vertex set of $\Gamma^{LR}(\text{SYM}_n, S)$ is SYM_n and there are two types of edges: for all $\pi, \pi' \in \text{SYM}_n$, there is an edge between π and π' labeled “ σ_i ” if $\sigma_i \cdot \pi = \pi'$ where $\sigma_i \in S$, and an edge between π and π' labeled “ $\cdot\sigma_j$ ” if $\pi \cdot \sigma_j = \pi'$ where $\sigma_j \in S$. Note in particular that this graph is not simple, as some pairs of vertices have two edges between them. We can now articulate the dual graph for $\text{MULT}_n(\mathbf{Q})$ as follows.

Theorem B (Theorem 3.10). *The dual graph of the bisimplicial cell structure on $\text{MULT}_n(\mathbf{Q})$ is isomorphic to $\Gamma^{LR}(\text{SYM}_n, S)$.*

Date: April 8, 2026.

Part of our interest in the space of rectangular multisets comes from its relationship to spaces of complex polynomials. In particular, if $\text{POLY}_{n+1}^{mc}(\mathbf{Q})$ denotes the space of monic degree- $(n+1)$ complex polynomials with roots centered at the origin and critical values confined to the closed rectangle \mathbf{Q} , then $\text{POLY}_{n+1}^{mc}(\mathbf{Q})$ can be endowed with a bisimplicial cell structure called the “branched rectangle complex” [DMb]. Moreover, the function which sends each complex polynomial to its multiset of critical values (known as the *Lyashko–Looijenga map*—see [LZ04] for a reference) is a cellular stratified covering map from $\text{POLY}_{n+1}^{mc}(\mathbf{Q})$ to $\text{MULT}_n(\mathbf{Q})$. In this sense, the cell structure defined in Theorem A gives rise to the cell structure on the space of complex polynomials with critical values confined to \mathbf{Q} , and as shown in [DMb], there is a quotient of this cell complex by face identifications which is homeomorphic to the space of monic polynomials with $n+1$ *distinct* centered roots, a classifying space for the $(n+1)$ -strand braid group.

The remainder of the article is structured as follows. Section 1 describes our conventions and definitions for permutations and orthoschemes. In Section 2, we examine the space of linear multisets and define the corresponding poset of linear compositions. We define the analogous space of rectangular multisets and the poset of rectangular compositions in Section 3, where we also provide the proofs of Theorem A and Theorem B. Finally, we provide some additional ways to illustrate bi-orthoschemes via spines in Section 4.

1. PERMUTATIONS AND ORTHOSCHEMES

In this section we give our conventions for permutations and review some basic facts about orthoschemes. Throughout this article, let $[n]$ denote the set $\{1, \dots, n\}$ where n is a positive integer.

Definition 1.1 (Permutations). Let S be a finite linearly ordered set, which we identify with $[n]$. Each permutation π in the symmetric group SYM_n can be viewed as a bijection between two copies of S : one on the left and one on the right. Moreover, π can be represented as a product of disjoint cycles $(a_1 a_2 \cdots a_k)$, each of which indicates that the element a_i in the left copy of S is sent to a_{i+1} in the right copy (with indices evaluated mod k). There are then two natural actions of a permutation $\pi \in \text{SYM}_n$ on S ; if $(a b c)$ is part of the disjoint cycle representation of π then the left action gives $\pi \cdot b = a$ (since b on the right is sent to a on the left) and the right action gives $b \cdot \pi = c$ (since b on the left is sent to c on the right). That is, the left action uses the right copy of S as its domain, and the right action uses the left copy of S as its domain. Finally, if σ_i is the transposition $(i i+1)$ for $i \in [n-1]$, then $\{\sigma_1, \dots, \sigma_{n-1}\}$ forms the standard generating set for SYM_n .

Permutations can also be represented as matrices of zeros and ones.

Definition 1.2 (Permutation matrices). A permutation π of $[n]$ can be represented as an $n \times n$ *permutation matrix* $M_\pi = (m_{ij})$ by setting $m_{ij} = 1$ if $i \cdot \pi = j$ and $m_{ij} = 0$ otherwise. Permutation composition corresponds to matrix multiplication in the sense that if $\alpha, \beta \in \text{SYM}_n$, then the permutation $\alpha\beta$ is represented by the matrix $M_\alpha M_\beta$. In particular, note that the matrix product $M_{\sigma_i} M_\pi$ is obtained from M_π by swapping rows i and $i+1$, whereas $M_\pi M_{\sigma_i}$ is obtained from M_π by swapping columns i and $i+1$. As a convenient visual shorthand, we can encode a permutation π using an $n \times n$ grid in which dots represent the positions of 1’s in M_π —see Figure 6.

Next, we define the metric simplices known as orthoschemes and describe their appearance in n -dimensional cubes.

Definition 1.3 (Orthoschemes and spines). Let $\mathbf{v}_1, \dots, \mathbf{v}_n$ be an orthogonal set of vectors in Euclidean space. Fix a point p_0 , and for each $i \in [n]$, define the point $p_i = p_0 + \mathbf{v}_1 + \mathbf{v}_2 + \dots + \mathbf{v}_i$. Then the convex hull of the points p_0, \dots, p_n is an n -dimensional orthoscheme. An orthoscheme is said to be *standard* if the vectors $\mathbf{v}_1, \dots, \mathbf{v}_n$ all have equal length. Finally, the *spine* of an orthoscheme is the subgraph of its 1-skeleton which consists of vertices p_0, \dots, p_n and edges e_1, \dots, e_n such that for all $i \in [n]$, e_i connects p_{i-1} to p_i .

Definition 1.4 (Cubes). Let $\mathbf{I} = [x_\ell, x_r]$ be a closed interval in \mathbb{R} with $x_\ell \neq x_r$. The n -cube $\mathbf{I}^n \subset \mathbb{R}^n$ inherits a simplicial cell structure from its intersection with the real braid arrangement, which consists of the $\binom{n}{2}$ hyperplanes described by equations of the form $x_i = x_j$ for distinct $i, j \in [n]$. The $n!$ top-dimensional cells are standard n -dimensional orthoschemes. The linear order on \mathbf{I} extends to a coordinate-by-coordinate partial order on \mathbf{I}^n . Under this partial order, the vertices of each simplex are totally ordered, and these *ordered simplices* turn \mathbf{I}^n into an *ordered simplicial complex*.

2. LINEAR MULTISSETS AND COMPOSITIONS

In this section we review the cell structure for the multiset space of a compact interval (isometric to a standard orthoscheme) and its associated face poset of linear compositions (isomorphic to a truncated Boolean lattice). For more details on the content of this section, see [DMa].

Definition 2.1 (Multiset spaces). Let X be a topological space and let n be a positive integer. As described in the introduction, the symmetric group SYM_n acts on X^n by permuting coordinates, and the quotient is the *multiset space* $\text{MULT}_n(X)$. Each point in this space is a *multiset* which can be represented either formally as a function $\mathbf{m}: X \rightarrow \mathbb{N}$ such that $\sum_{x \in X} \mathbf{m}(x) = n$ (necessitating that $\mathbf{m}(x) = 0$ for all but finitely many $x \in X$) or informally as a collection of n points in X where multiplicity is permitted. Note that the multiset space $\text{MULT}_n(X)$ is distinct from the related configuration space $\text{CONF}_n(X)$ (in which points are subsets of X with n elements) and subset space $\text{exp}_n(X)$ (in which points are subsets of X with at most n elements); see e.g. [Tuf02] for a comparison of the latter two cases.

Definition 2.2 (Linear multisets). Let $\mathbf{I} = [x_\ell, x_r]$ as in Definition 1.4. The symmetric group SYM_n acts on \mathbf{I}^n by permuting coordinates in two ways: for each $\sigma \in \text{SYM}_n$ and $\mathbf{x} = (x_1, x_2, \dots, x_n)$ in \mathbf{I}^n , define the left action $\sigma \cdot \mathbf{x} = (x_{\sigma^{-1}}, x_{\sigma^{-2}}, \dots, x_{\sigma^{-n}})$ and the right action $\mathbf{x} \cdot \sigma = (x_{n, \sigma}, \dots, x_{2, \sigma}, x_{1, \sigma})$. In both cases, the action preserves the ordering on each simplex, and the multiset space $\text{MULT}_n(\mathbf{I})$ is a single ordered n -dimensional orthoscheme.

Each linear multiset $\mathbf{x} \in \text{MULT}_n(\mathbf{I})$ can be uniquely denoted with the shorthand notation $\mathbf{x} = x_\ell^{m_\ell} x_1^{m_1} \dots x_k^{m_k} x_r^{m_r}$, where $x_\ell < x_1 < \dots < x_k < x_r$ in \mathbf{I} and m_i denotes the multiplicity of x_i in \mathbf{x} . Note that this notation always includes the endpoints of \mathbf{I} , even if they do not appear in \mathbf{x} ; in other words, m_ℓ and m_r may be zero, while m_1, \dots, m_k are strictly positive. As for the cell structure, the simplices in $\text{MULT}_n(\mathbf{I})$ admit a natural labeling by compositions of n in the following sense.

Definition 2.3 (Linear compositions). Let n be a positive integer and let k be a nonnegative integer. A *linear composition of n with length $k + 2$* is a row vector $\mathbf{a} = [a_\ell \ a_1 \ \cdots \ a_k \ a_r]$ of integers with entry sum n such that $a_\ell = a_0$ and $a_r = a_{k+1}$ are nonnegative, and every other a_i is positive for $i \in [k]$. A composition of length $k + 2$ can be *merged* at position $i \in [k + 1]$ by replacing the two entries a_{i-1} and a_i with the single entry $a_{i-1} + a_i$ to obtain a new composition of n with length $k + 1$. Let $\text{COMP}_n(\longleftrightarrow)$ denote the set of all linear compositions of n together with the partial order $\mathbf{a} \leq \mathbf{b}$ if there is a sequence of merges which can be applied to \mathbf{b} to obtain \mathbf{a} . Note that if \mathbf{a} is a vector of length $k + 2$ with nonnegative integer entries which sum to n , then \mathbf{a} is a linear composition of n if and only if none of its internal (i.e. non-first, non-last) entries are zero.

Note that $\text{COMP}_n(\longleftrightarrow)$ has a unique maximum element $[0 \ 1 \ \cdots \ 1 \ 0]$ and each element below it is determined by performing a subset of the $n + 1$ possible merges. In other words, $\text{COMP}_n(\longleftrightarrow)$ is isomorphic to BOOL_{n+1}^* , the Boolean lattice with its minimum element removed. Although BOOL_{n+1}^* has a more natural definition as the nonempty subsets of $[n + 1]$, our definition for $\text{COMP}_n(\longleftrightarrow)$ provides a direct connection with the set of multisets in \mathbf{I} .

Define the surjective map $\text{COMP}: \text{MULT}_n(\mathbf{I}) \rightarrow \text{COMP}_n(\longleftrightarrow)$ by

$$\text{COMP}(x_\ell^{m_\ell} x_1^{m_1} \cdots x_k^{m_k} x_r^{m_r}) = [m_\ell \ m_1 \ \cdots \ m_k \ m_r]$$

and recall that the *face poset* of a polyhedral cell complex is the set of all nonempty faces, partially ordered by inclusion (see e.g. [Wac07]). We then have the following proposition.

Proposition 2.4 ([DMa, Example 4.4]). *The face poset for $\text{MULT}_n(\mathbf{I})$ is isomorphic to $\text{COMP}_n(\longleftrightarrow)$.*

Proof. The preimage of each linear composition of n under the COMP map is an open cell in $\text{MULT}_n(\mathbf{I})$, and $\mathbf{a} \leq \mathbf{b}$ in $\text{COMP}_n(\longleftrightarrow)$ if and only if $\text{COMP}^{-1}(\mathbf{a})$ is a subset of the closure of $\text{COMP}^{-1}(\mathbf{b})$. Thus, each face of $\text{MULT}_n(\mathbf{I})$ is uniquely labeled by a linear composition of n , and the partial order of merging in $\text{COMP}_n(\longleftrightarrow)$ corresponds exactly to the inclusion of faces in $\text{MULT}_n(\mathbf{I})$. \square

See Figure 1 for an illustration of the 3-dimensional orthoscheme $\text{MULT}_3(\mathbf{I})$ with cells labeled by the linear compositions of 3. To close this section, we note some useful ways of visualizing the space of linear multisets and the corresponding linear compositions.

Remark 2.5 (Illustrating orthoschemes). Given a multiset $\mathbf{x} \in \text{MULT}_n(\mathbf{I})$, it is easy to read off not only the linear composition $\text{COMP}(\mathbf{x})$, but also the linear compositions which label the vertices of the corresponding orthoscheme: each vertex label is obtained by preserving a single gap between entries and merging at all other positions in $\text{COMP}(\mathbf{x})$. For example, if $\mathbf{x} = x_\ell^3 x_1^4 x_2^1 x_3^2 x_r^1 \in \text{MULT}_{11}(\mathbf{I})$, then \mathbf{x} lies in the interior of the 3-dimensional orthoscheme labeled by the linear composition $\text{COMP}(\mathbf{x}) = [3 \ 4 \ 1 \ 2 \ 1]$, and the spine of this orthoscheme goes through the vertices $[3 \ 8]$, $[7 \ 4]$, $[8 \ 3]$ and $[10 \ 1]$, in order. Moreover, the multiplicities of x_1 , x_2 and x_3 tell us that the edges connecting these vertices are of lengths $\sqrt{4}$, $\sqrt{1}$, and $\sqrt{2}$ respectively. See Figure 2 for an illustration which overlays the spine of the orthoscheme labeled by $\text{COMP}(\mathbf{x})$ on the multiset \mathbf{x} .

convention established in Remark 3.1, we think of \mathbf{I} as blue and \mathbf{J} as red. The n -fold product \mathbf{Q}^n can then be viewed as the product of a blue n -cube \mathbf{I}^n and a red n -cube \mathbf{J}^n , each of which has a simplicial cell structure from Definition 2.2. The result is a bisimplicial cell structure on \mathbf{Q}^n with $(n!)^2$ top-dimensional cells, each of which is the product of two n -dimensional orthoschemes (one blue, one red). The action of SYM_n on \mathbf{Q}^n by permuting coordinates can be viewed as the diagonal action on $\mathbf{I}^n \times \mathbf{J}^n$ which restricts to the action from Definition 2.2 on each coordinate, and the quotient $\text{MULT}_n(\mathbf{Q})$ is a cell complex with $n!$ top-dimensional cells.

Viewing \mathbf{Q} as a subset of the complex plane, the projection maps onto real and imaginary parts give us projections $\Re: \mathbf{Q} \rightarrow \mathbf{I}$ and $\Im: \mathbf{Q} \rightarrow \mathbf{J}$, and they naturally extend to projections $\Re: \text{MULT}_n(\mathbf{Q}) \rightarrow \text{MULT}_n(\mathbf{I})$ and $\Im: \text{MULT}_n(\mathbf{Q}) \rightarrow \text{MULT}_n(\mathbf{J})$. Each multiset $\mathbf{z} \in \text{MULT}_n(\mathbf{Q})$ uniquely determines the pair $(\mathbf{x}, \mathbf{y}) = (\Re(\mathbf{z}), \Im(\mathbf{z}))$, and we denote \mathbf{x} and \mathbf{y} as

$$\begin{aligned} \mathbf{x} &= x_\ell^{c_\ell} x_1^{c_1} \cdots x_h^{c_h} x_r^{c_r} && (x_\ell < x_1 < \cdots < x_h < x_r) \\ \mathbf{y} &= y_b^{d_b} y_1^{d_1} \cdots y_k^{d_k} y_t^{d_t} && (y_b < y_1 < \cdots < y_k < y_t). \end{aligned}$$

As noted in Section 2, the endpoints x_ℓ , x_r , y_b and y_t appear in the notation for \mathbf{x} and \mathbf{y} even if they are not elements of those multisets; the exponents for those entries may be zero. Moreover, the map $\text{MULT}_n(\mathbf{Q}) \rightarrow \text{MULT}_n(\mathbf{I}) \times \text{MULT}_n(\mathbf{J})$ given by $\mathbf{z} \mapsto (\mathbf{x}, \mathbf{y})$ is a cellular surjection, and each point in the interior of $\text{MULT}_n(\mathbf{I}) \times \text{MULT}_n(\mathbf{J})$ has exactly $n!$ preimages in $\text{MULT}_n(\mathbf{Q})$. More generally, the number of preimages can be enumerated by counting certain types of matrices with specified row sums and column sums.

As in the case of linear multisets, the higher-dimensional cells of $\text{MULT}_n(\mathbf{Q})$ can be understood using a convenient combinatorial tool. To smooth the transition from multisets in planar rectangles to integers in matrices, we need to navigate a discrepancy between planar conventions and matrix conventions.

Remark 3.4 (Reconciling orientations). The standard planar coordinate system with points (x, y) has the positive x -axis pointing to the right and the positive y -axis pointing upwards. The standard discrete matrix coordinate system has entries (i, j) with the row index i increasing as one descends vertically, and the column index j increasing as one moves to the right. To reconcile the differences between these two conventions, we choose to rotate the plane clockwise by a quarter-turn so that it appears in “matrix orientation” (with the positive x -axis pointing downward and the positive y -axis pointing to the right). See the lefthand side of Figure 3, where the planar rectangle \mathbf{Q} is shown in “matrix orientation”. In fact, matrix orientation is used consistently in all of the figures. Our color conventions (Remark 3.1) remain based on “planar orientation”.

Remark 3.5 (Multiplicity matrix). For each rectangular multiset \mathbf{z} of n points in the rectangle \mathbf{Q} , we define a *multiplicity matrix* that records the multiplicities of points in \mathbf{z} , with entry sum n . We use the natural order of the reals in the intervals $\mathbf{I} = [x_\ell, x_r]$ and $\mathbf{J} = [y_b, y_t]$ to index the rows and columns respectively. When the rectangle \mathbf{Q} is viewed in matrix orientation (Remark 3.4), the multiset in \mathbf{Q} visually aligns with the multiplicity matrix. Figure 3 illustrates the process: the multiset \mathbf{z} contains a point of multiplicity 1 at the point (x_1, y_t) in \mathbf{Q} , so the corresponding matrix $\text{COMP}(\mathbf{z})$ has a 1 in the $(2, 4)$ -entry.

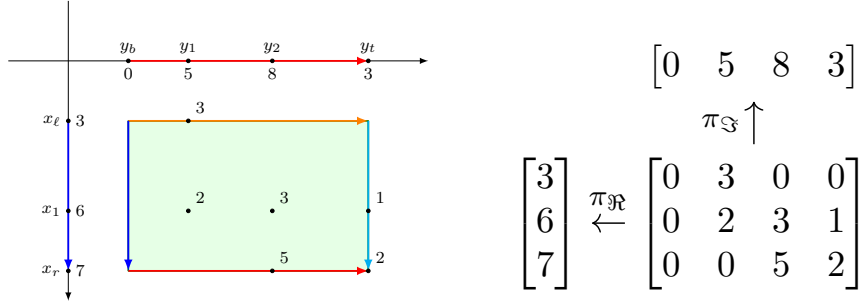


FIGURE 3. On the left, an element $\mathbf{z} \in \text{MULT}_{16}(\mathbf{Q})$ along with its projections $\mathbf{x} = \mathfrak{R}(\mathbf{z}) = x_\ell^3 x_1^6 x_r^7$ and $\mathbf{y} = \mathfrak{S}(\mathbf{z}) = y_b^0 y_1^5 y_2^8 y_t^3$. The labels on each point in \mathbf{Q} correspond to the multiplicity of that point in \mathbf{z} . On the right, the rectangular composition $\text{COMP}(\mathbf{z})$ along with the linear compositions $\text{COMP}(\mathbf{x})$ and $\text{COMP}(\mathbf{y})$.

Definition 3.6 (Rectangular compositions). Let n be a positive integer and let k and l be nonnegative integers. Given an $(h+2) \times (k+2)$ matrix

$$\mathbf{a} = \begin{bmatrix} a_{\ell,b} & a_{\ell,1} & \cdots & a_{\ell,k} & a_{\ell,t} \\ a_{1,b} & a_{1,1} & \cdots & a_{1,k} & a_{1,t} \\ \vdots & \vdots & \ddots & \vdots & \vdots \\ a_{h,b} & a_{h,1} & \cdots & a_{h,k} & a_{h,t} \\ a_{r,b} & a_{r,1} & \cdots & a_{r,k} & a_{r,t} \end{bmatrix}$$

of nonnegative integers, let $c_\ell, c_1, \dots, c_h, c_r$ denote the row sums of \mathbf{a} and let $d_b, d_1, \dots, d_k, d_t$ denote the column sums of \mathbf{a} . We say that \mathbf{a} is a *rectangular composition of n with shape $(h+2) \times (k+2)$* if

- (1) $c_i > 0$ for all $i \in [h]$ (c_ℓ and c_r can be zero);
- (2) $d_j > 0$ for all $j \in [k]$ (d_t and d_b can be zero);
- (3) $c_\ell + c_1 + \cdots + c_h + c_r = n$.

A rectangular composition can be *row-merged* (resp. *column-merged*) to obtain a new rectangular composition of n with shape $(h+1) \times (k+2)$ (resp. $(h+2) \times (k+1)$) by removing two adjacent rows (resp. columns) and inserting their sum. Let $\text{COMP}_n(\square)$ denote the set of all rectangular compositions of n and define a partial order by declaring $\mathbf{a} \leq \mathbf{a}'$ if and only if there is a sequence of row-merges and/or column-merges which transforms \mathbf{a}' into \mathbf{a} . Finally, note that if \mathbf{a} is an $(h+2) \times (k+2)$ matrix with nonnegative integer entries which sum to n , then \mathbf{a} is a rectangular composition of n if and only if it has no internal rows or internal columns which sum to zero.

The multiplicities of an n -multiset in a rectangle \mathbf{Q} determine a rectangular composition of n in the following sense. Given $\mathbf{z} \in \text{MULT}_n(\mathbf{Q})$, let $(\mathbf{x}, \mathbf{y}) = (\mathfrak{R}(\mathbf{z}), \mathfrak{S}(\mathbf{z}))$ as above, and for each $i \in \{\ell, 1, \dots, h, r\}$ and $j \in \{b, 1, \dots, k, t\}$, define $m_{i,j} \geq 0$ to

be the multiplicity of (x_i, y_j) in \mathbf{z} . Then we define

$$\text{COMP}(\mathbf{z}) = \begin{bmatrix} m_{\ell,b} & m_{\ell,1} & \cdots & m_{\ell,k} & m_{\ell,t} \\ m_{1,b} & m_{1,1} & \cdots & m_{1,k} & m_{1,t} \\ \vdots & \vdots & \ddots & \vdots & \vdots \\ m_{h,b} & m_{h,1} & \cdots & m_{h,k} & m_{h,t} \\ m_{r,b} & m_{r,1} & \cdots & m_{r,k} & m_{r,t} \end{bmatrix}$$

and observe that this defines a surjective map $\text{COMP}: \text{MULT}_n(\mathbf{Q}) \rightarrow \text{COMP}_n(\square)$.

The $n!$ maximal elements of $\text{COMP}_n(\square)$ are all of shape $(n+2) \times (n+2)$ and can be viewed as $n \times n$ permutation matrices which have been padded with zeros along the outside. The minimal elements of $\text{COMP}_n(\square)$ are 2×2 matrices with entries in $\{0, 1, \dots, n\}$ and sum n , and these are counted by the *tetrahedral numbers* $\binom{n+3}{3}$. To see why, note that these 2×2 matrices are in one-to-one correspondence with the integer lattice points in \mathbb{R}^4 which lie on the tetrahedron formed by the intersection of the hyperplane $x_1 + x_2 + x_3 + x_4 = n$ with the positive orthant.

Each rectangular composition determines a pair of linear compositions, and these are compatible with the projection maps $\mathfrak{R}: \text{MULT}_n(\mathbf{Q}) \rightarrow \text{MULT}_n(\mathbf{I})$ and $\mathfrak{S}: \text{MULT}_n(\mathbf{Q}) \rightarrow \text{MULT}_n(\mathbf{J})$ described above.

Definition 3.7 (Composition projections). There are two natural projection maps $\text{COMP}_n(\square) \rightarrow \text{COMP}_n(\blackrightarrow)$. If $\mathbf{z} \in \text{MULT}_n(\mathbf{Q})$ with $\mathbf{a} = \text{COMP}(\mathbf{z})$ the corresponding rectangular composition of n , then we define $\pi_{\mathfrak{R}}(\mathbf{a}) = \pi_{\mathfrak{R}}(\text{COMP}(\mathbf{z})) = \text{COMP}(\mathfrak{R}(\mathbf{z}))$ and $\pi_{\mathfrak{S}}(\mathbf{a}) = \pi_{\mathfrak{S}}(\text{COMP}(\mathbf{z})) = \text{COMP}(\mathfrak{S}(\mathbf{z}))$. In other words, if \mathbf{a} has row sums $c_\ell, c_1, \dots, c_h, c_r$ and column sums $d_b, d_1, \dots, d_k, d_t$, then $\pi_{\mathfrak{R}}(\mathbf{a}) = [c_\ell \ c_1 \ \cdots \ c_h \ c_r]$ and $\pi_{\mathfrak{S}}(\mathbf{a}) = [d_b \ d_1 \ \cdots \ d_k \ d_t]$. Moreover, recall that if \mathbf{a} is an $(h+2) \times (k+2)$ matrix with nonnegative integer entries that sum to n , then \mathbf{a} is a rectangular composition if and only if it has no internal rows or internal columns which sum to zero; this is equivalent to saying that the projections $\pi_H(\mathbf{a})$ and $\pi_V(\mathbf{a})$ have no internal entries of zero, which is in turn equivalent to $\pi_H(\mathbf{a})$ and $\pi_V(\mathbf{a})$ being linear compositions of n .

Analogous to the case of linear compositions, we have the following theorem.

Theorem 3.8 (Theorem A). $\text{COMP}_n(\square)$ is the face poset for $\text{MULT}_n(\mathbf{Q})$.

Proof. As described in Definition 3.3, each open cell in $\text{MULT}_n(\mathbf{Q})$ can be viewed as the product of an open blue orthoscheme and an open red orthoscheme. If $\mathbf{z} \in \text{MULT}_n(\mathbf{Q})$, then the projections $\mathfrak{R}(\mathbf{z})$ and $\mathfrak{S}(\mathbf{z})$ label points in the blue and red factor orthoschemes, respectively. We can then deform \mathbf{z} by fixing $\mathfrak{S}(\mathbf{z})$ and allowing $\mathfrak{R}(\mathbf{z})$ to vary without intersections; these deformed points have the same label in the red factor, but produce all possible points in the blue factor. Analogously, fixing $\mathfrak{R}(\mathbf{z})$ while varying $\mathfrak{S}(\mathbf{z})$ produces all possible points in the red orthoscheme while fixing the point in the blue orthoscheme. Since these two deformations can be performed independently, we can obtain all points in the open cell containing $\text{MULT}_n(\mathbf{Q})$ in this manner, and it is clear that $\text{COMP}(\mathbf{z})$ remains constant throughout. Moreover, we obtain all points in the preimage $\text{COMP}^{-1}(\text{COMP}(\mathbf{z}))$ through these deformations. In other words, the preimage of each rectangular composition of n under the map $\text{COMP}: \text{MULT}_n(\mathbf{Q}) \rightarrow \text{COMP}_n(\square)$ is an open bisimplex.

Furthermore, $\mathbf{a} \leq \mathbf{b}$ in $\text{COMP}_n(\square)$ if and only if \mathbf{a} can be obtained from \mathbf{b} by a sequence of row-merges and/or column-merges. If we consider $\text{COMP}^{-1}(\mathbf{b})$

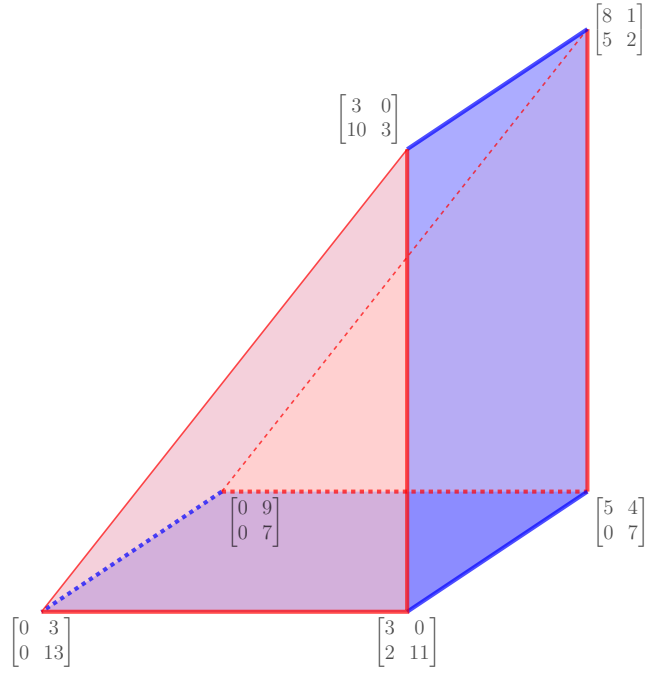


FIGURE 4. The bi-orthoscheme labeled by the rectangular composition defined in Remark 3.9 (the direct product of a red triangle with a blue line segment) with vertex set labeled. The spine of this bi-orthoscheme, consisting of two rectangular faces along with their seven edges and six vertices, is highlighted.

as a product of a blue orthoscheme and a red orthoscheme, then each row-merge (resp. column-merge) corresponds to replacing the blue orthoscheme (resp. red orthoscheme) with one of its facets, so the resulting open bisimplex $\text{COMP}^{-1}(\mathbf{a})$ is a subset of the closure of $\text{COMP}^{-1}(\mathbf{b})$. Since each cell of $\text{MULT}_n(\mathbf{Q})$ can thus be labeled by a unique rectangular composition in a manner which respects the incidence of cells, the proof is complete. \square

There are many useful ways of illustrating bi-orthoschemes, some of which are described in the following remark.

Remark 3.9 (Illustrating bi-orthoschemes). Similar to the case for multisets in a line segment presented in Remark 2.5, it is straightforward to read off the labels for the bi-orthoscheme containing a given multiset $\mathbf{z} \in \text{MULT}_n(\mathbf{Q})$ and all of its faces. In Figure 3, we see that a multiset in $\text{MULT}_{16}(\mathbf{Q})$ and its projections immediately determine the corresponding rectangular composition and projected linear compositions. The rectangular composition $\text{COMP}(\mathbf{z})$ labels a triangular prism in the cell structure for $\text{MULT}_{16}(\mathbf{Q})$, depicted in Figure 4 as the product of a red 2-orthoscheme with label $[0\ 5\ 8\ 3]$ (i.e. a right triangle with legs of length $\sqrt{5}$ and $\sqrt{8}$) and a blue 1-orthoscheme with label $[3\ 6\ 7]$ (i.e. an edge with length $\sqrt{6}$). For the full face poset of this cell, we can take the subposet of $\text{COMP}_{16}(\square)$ consisting of all elements below $\text{COMP}(\mathbf{z})$, illustrated in Figure 5.

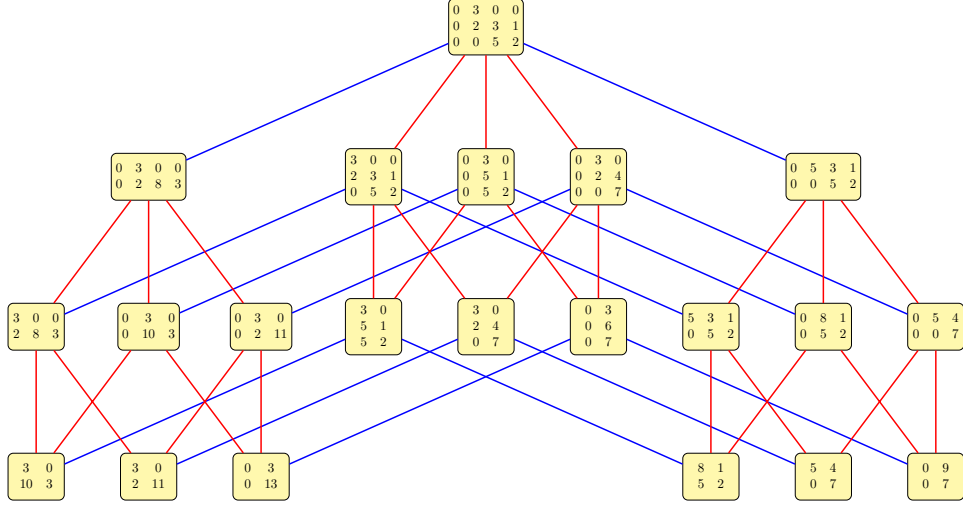


FIGURE 5. The elements in $\text{COMP}_{16}(\square)$ below the fixed rectangular composition defined in Remark 3.9. The blue edges in the order diagram correspond to row-merges and the red edges correspond to column-merges.

Next, we describe the structure of the top-dimensional cells in $\text{MULT}_n(\mathbf{Q})$ by proving Theorem B. Recall from the Introduction that $\Gamma^{LR}(\text{SYM}_n, S)$ is the graph obtained by overlaying the left and right Cayley graphs of SYM_n on a common vertex set.

Theorem 3.10 (Theorem B). *The dual graph of the bisimplicial cell structure on $\text{MULT}_n(\mathbf{Q})$ is isomorphic to $\Gamma^{LR}(\text{SYM}_n, S)$.*

Proof. The top-dimensional cells of $\text{MULT}_n(\mathbf{Q})$ are labeled by the maximal elements of $\text{COMP}_n(\square)$, which are the $(n + 2) \times (n + 2)$ matrices formed by padding an $n \times n$ permutation matrix with zeros on all four sides. Thus, each vertex of the dual graph can be uniquely labeled by an element of SYM_n , which we represent with an $n \times n$ permutation matrix.

Two top-dimensional cells of $\text{MULT}_n(\mathbf{Q})$ share a face of codimension one if and only if the two corresponding permutation matrices can be obtained from one another via a single swap of two rows or two columns. Swapping rows i and $i + 1$ corresponds to left multiplication by the permutation matrix for the transposition $(i \ i + 1)$, whereas swapping columns i and $i + 1$ corresponds to right multiplication by the same matrix. This means that the edges of the dual graph come from both the left and right Cayley graphs of SYM_n with respect to the standard generating set of adjacent transpositions, and the proof is complete. \square

To clarify any confusion regarding the two actions by SYM_n , consider the following example of applying the transposition $\sigma_2 = (2 \ 3)$ to the left and right of a 5×5

permutation matrix:

$$\sigma_2 \cdot \begin{bmatrix} 0 & 0 & 0 & 1 & 0 \\ 1 & 0 & 0 & 0 & 0 \\ 0 & 0 & 0 & 0 & 1 \\ 0 & 1 & 0 & 0 & 0 \\ 0 & 0 & 1 & 0 & 0 \end{bmatrix} = \begin{bmatrix} 0 & 0 & 0 & 1 & 0 \\ 0 & 0 & 0 & 0 & 1 \\ 1 & 0 & 0 & 0 & 0 \\ 0 & 1 & 0 & 0 & 0 \\ 0 & 0 & 1 & 0 & 0 \end{bmatrix}$$

and

$$\begin{bmatrix} 0 & 0 & 0 & 1 & 0 \\ 1 & 0 & 0 & 0 & 0 \\ 0 & 0 & 0 & 0 & 1 \\ 0 & 1 & 0 & 0 & 0 \\ 0 & 0 & 1 & 0 & 0 \end{bmatrix} \cdot \sigma_2 = \begin{bmatrix} 0 & 0 & 0 & 1 & 0 \\ 1 & 0 & 0 & 0 & 0 \\ 0 & 0 & 0 & 0 & 1 \\ 0 & 0 & 1 & 0 & 0 \\ 0 & 1 & 0 & 0 & 0 \end{bmatrix}.$$

Each matrix can also be viewed with a representative generic configuration of five dots in \mathbf{Q} ; in this perspective, keeping in mind the matrix orientation described in Remark 3.4, the left action permutes the ordering of points in the x direction, whereas the right action permutes the y coordinates. In Figure 6, we provide an illustration of the full dual graph for $\text{MULT}_3(\mathbf{Q})$.

A more robust picture can be obtained by looking at the full dual complex of $\text{MULT}_n(\mathbf{Q})$ rather than just the dual graph. If \mathbf{I}^n is an n -dimensional cube, subdivided into $n!$ standard n -dimensional orthoschemes as in Definition 1.4, then the dual complex of this cell structure is a simple convex polytope called the $(n-1)$ -dimensional *permutahedron*, and it can be defined as the convex hull of the orbit of a generic configuration under the (left) action of SYM_n on \mathbf{I}^n . The 1-skeleton of the permutahedron is then the (right) Cayley graph of SYM_n with respect to the standard generating set of adjacent transpositions.

For example, if $\mathbf{I} = [0, 4]$ and $\mathbf{x} = (1, 2, 3)$, then \mathbf{I}^3 is subdivided into six standard 3-dimensional orthoschemes, each of which contains one point in the orbit of \mathbf{x} under the (left) action of SYM_3 in its interior. All six points lie on the plane $x + y + z = 6$, and their convex hull is a regular hexagon with sides of length $\sqrt{2}$. The vertices and edges of this hexagon form the (right) Cayley graph of SYM_3 with respect to the generating set $\{\sigma_1, \sigma_2\}$.

It follows that the product $\mathbf{Q}^n = \mathbf{I}^n \times \mathbf{J}^n$ has a dual complex which is the direct product of two $(n-1)$ -dimensional permutahedra: a blue permutahedron dual to the simplicial structure on \mathbf{I}^n and a red permutahedron dual to the simplicial structure on \mathbf{J}^n . The coordinate-permuting action of SYM_n on \mathbf{Q}^n corresponds to the diagonal action on the product $\mathbf{I}^n \times \mathbf{J}^n$, with $\text{MULT}_n(\mathbf{Q})$ as the quotient. The dual complex for $\text{MULT}_n(\mathbf{Q})$ is thus the quotient of the product of two $(n-1)$ -dimensional permutahedra by the diagonal action of SYM_n .

4. BI-ORTHOSCHEME SPINES

In Definition 1.3, we defined the *spine* of an n -dimensional orthoscheme to be the subgraph of its 1-skeleton which contains all $n+1$ vertices, along with the n edges which connect one vertex to the next in the linear ordering. In Definition 3.2, we defined the *spine* of a bi-orthoscheme to be the subcomplex of its 2-skeleton which is formed by the product of the spines of the two factor simplices. Geometrically, the spine of an orthoscheme is a line segment, and the spine of a bi-orthoscheme is a rectangle. See Figure 7 for an example, noting how the spine can be overlaid

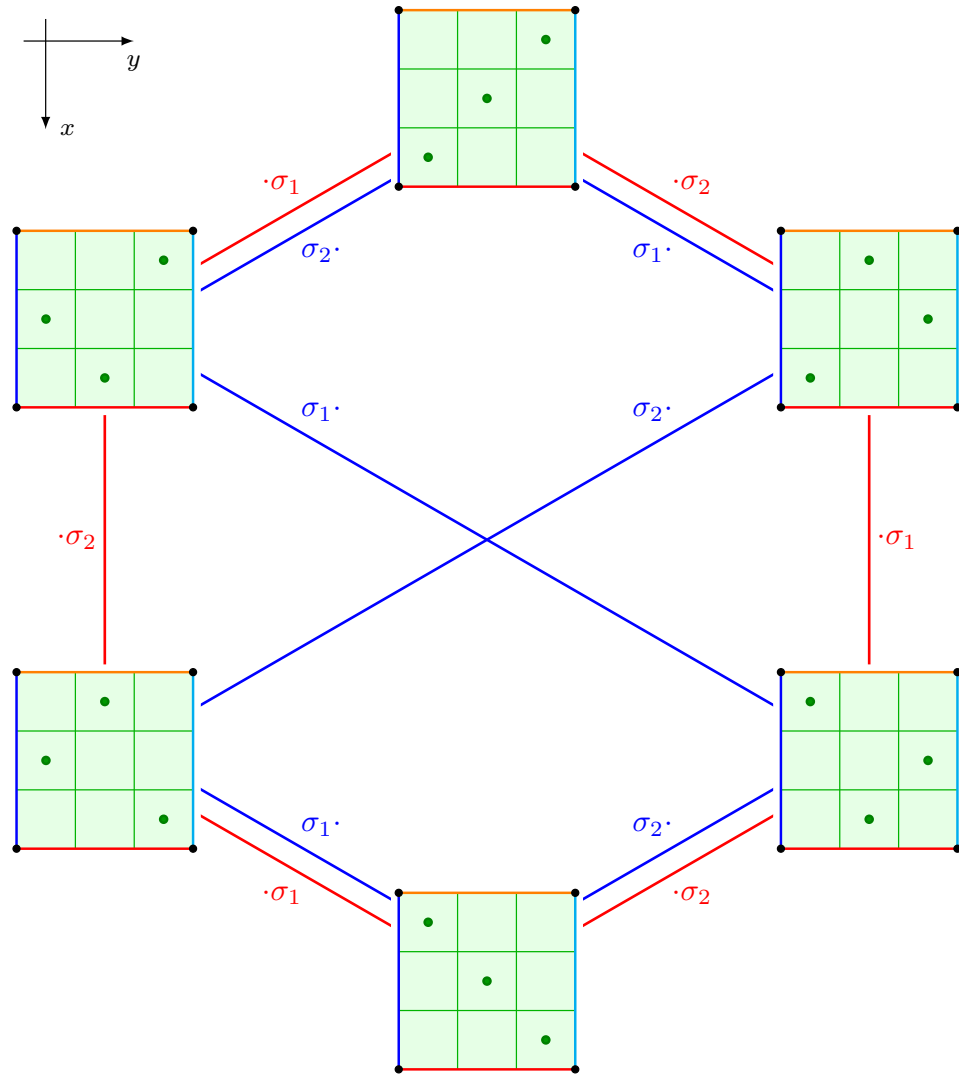


FIGURE 6. The dual graph for $\text{MULT}_3(\mathbf{Q})$ can be viewed as the superposition of the left and right Cayley graphs for SYM_3 with respect to the standard generating set $\{\sigma_1, \sigma_2\}$. The vertices of the graph are labeled by generic configurations representing the top-dimensional cells in $\text{MULT}_3(\mathbf{Q})$, from which the corresponding permutation matrix can be read off by replacing dots with ones and blank squares with zeros. The axes in the upper left serve as a reminder that each vertex is illustrated using a plane which has been rotated to accommodate the matrix orientation.

on top of a representative rectangular multiset \mathbf{z} so that each 2×2 matrix $\begin{bmatrix} a & b \\ c & d \end{bmatrix}$ (labeling a vertex of the bi-orthoscheme spine) is placed at a point where there are a elements of \mathbf{z} to the upper left, b to the upper right, c to the lower left, and d to

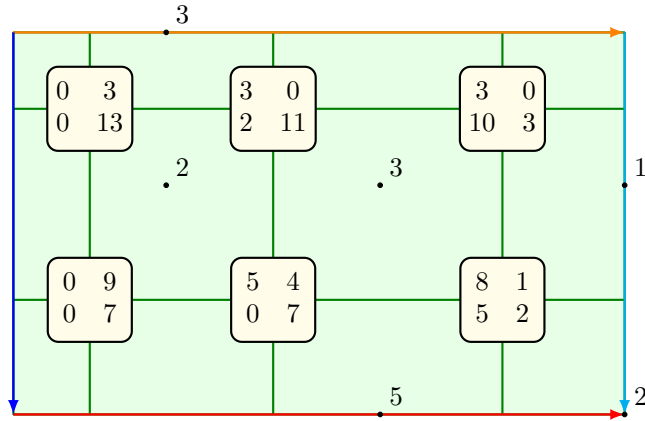


FIGURE 7. The multiset $\mathbf{z} \in \text{MULT}_{16}(\mathbf{Q})$ defined in Remark 3.9, with the corresponding bi-orthoscheme spine (which consists of six vertices, seven edges, and two rectangles) overlaid. The same spine is indicated with bold edges in Figure 4.

the lower right. In this manner, the entire spine of a bi-orthoscheme in $\text{MULT}_n(\mathbf{Q})$ can be easily read off of any point in its interior.

The spines of top-dimensional bi-orthoschemes are worth discussing separately.

Remark 4.1 (Top-dimensional spines). See Figure 8 for a generic configuration \mathbf{z} of 4 points in \mathbf{Q} and observe that it lies in the interior of the bi-orthoscheme in $\text{MULT}_4(\mathbf{Q})$ which is labeled by the rectangular composition

$$\text{COMP}(\mathbf{z}) = \begin{bmatrix} 0 & 0 & 0 & 0 & 0 & 0 \\ 0 & 0 & 1 & 0 & 0 & 0 \\ 0 & 0 & 0 & 1 & 0 & 0 \\ 0 & 1 & 0 & 0 & 0 & 0 \\ 0 & 0 & 0 & 0 & 1 & 0 \\ 0 & 0 & 0 & 0 & 0 & 0 \end{bmatrix}$$

in $\text{COMP}_4(\square)$. In the same figure, we see the spine of the bi-orthoscheme labeled by $\text{COMP}(\mathbf{z})$ with the four elements of \mathbf{z} superimposed. Note in particular that each edge of the spine corresponds to moving 1 from one entry to another in the same row or column, so each edge has a well-defined color depending on which column or row was left fixed: blue for fixing the left column, cyan for the right column, red for the bottom row, and orange for the top row. Furthermore, we can observe that the points in \mathbf{z} correspond to the squares in the spine with four distinct edge colors.

Finally, we note that all of the spines for the top-dimensional bi-orthoschemes are visible in a single 3-dimensional graph.

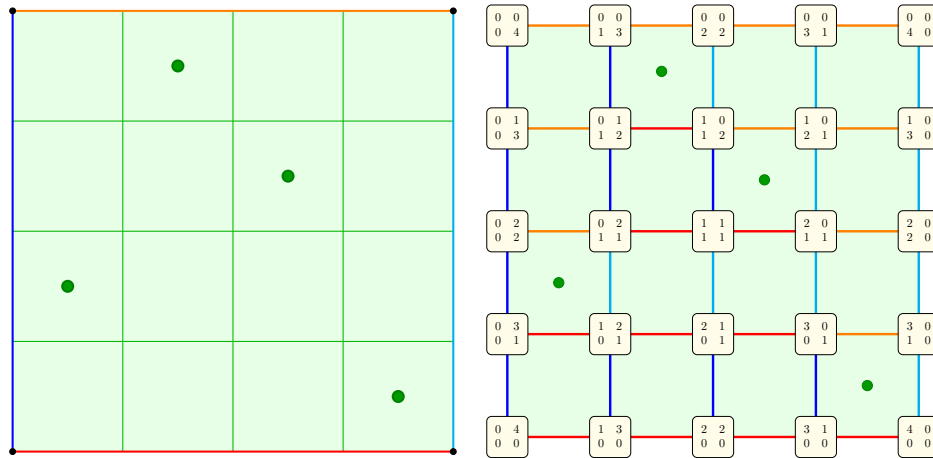


FIGURE 8. On the left, a generic configuration \mathbf{z} of four distinct points in \mathbf{Q} . On the right, the same configuration along with the spine of its corresponding bi-orthoscheme overlaid.

Remark 4.2 (Spines in a tetrahedral graph). In Section 3 we noted that the vertices of $\text{MULT}_n(\mathbf{Q})$ correspond to the positive integer lattice points in the hyperplane $x_1 + x_2 + x_3 + x_4 = n$. In Figure 9 we have placed the vertices according to their location in this tetrahedron with $n = 4$, and we have drawn some edges connecting them. In particular, we have drawn an edge when two vertex labels differ by moving one unit from an entry in the 2×2 matrix to another in the same row or column. This means that the 1-skeleton of the spine of any top-dimensional bi-orthoscheme is visible in this graph (Remark 4.1). For example, the spine from Figure 8 is highlighted in Figure 10. Notice that the vertices labeled by 2×2 matrices with either a row or a column of zeros form a cyclic graph with $4n$ edges, and that all of the top-dimensional spines contain this cycle of edges.

REFERENCES

- [DMa] Michael Dougherty and Jon McCammond, *Continuous noncrossing partitions and weighted circular factorizations*, Preprint 2025. [arXiv:2507.00283](#).
- [DMb] ———, *Geometric combinatorics of polynomials II: Polynomials and cell structures*, Preprint 2024. [arXiv:2410.03047](#).
- [LZ04] Sergei K. Lando and Alexander K. Zvonkin, *Graphs on surfaces and their applications*, Encyclopaedia of Mathematical Sciences, vol. 141, Springer-Verlag, Berlin, 2004, With an appendix by Don B. Zagier, Low-Dimensional Topology, II. MR 2036721
- [Tuf02] Christopher Tuffley, *Finite subset spaces of S^1* , *Algebr. Geom. Topol.* **2** (2002), 1119–1145. MR 1998017
- [Wac07] Michelle L. Wachs, *Poset topology: tools and applications*, Geometric combinatorics, IAS/Park City Math. Ser., vol. 13, Amer. Math. Soc., Providence, RI, 2007, pp. 497–615. MR 2383132

Email address: doughemj@lafayette.edu

DEPARTMENT OF MATHEMATICS, LAFAYETTE COLLEGE, EASTON, PA 18042

Email address: jon.mccammond@math.ucsb.edu

DEPARTMENT OF MATHEMATICS, UC SANTA BARBARA, SANTA BARBARA, CA 93106

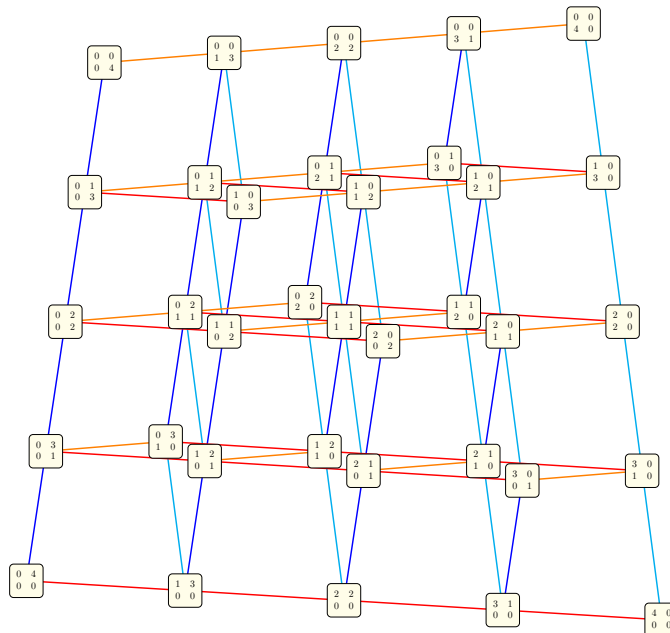


FIGURE 9. The tetrahedral graph of the multiset space $MULT_4(\mathbf{Q})$.

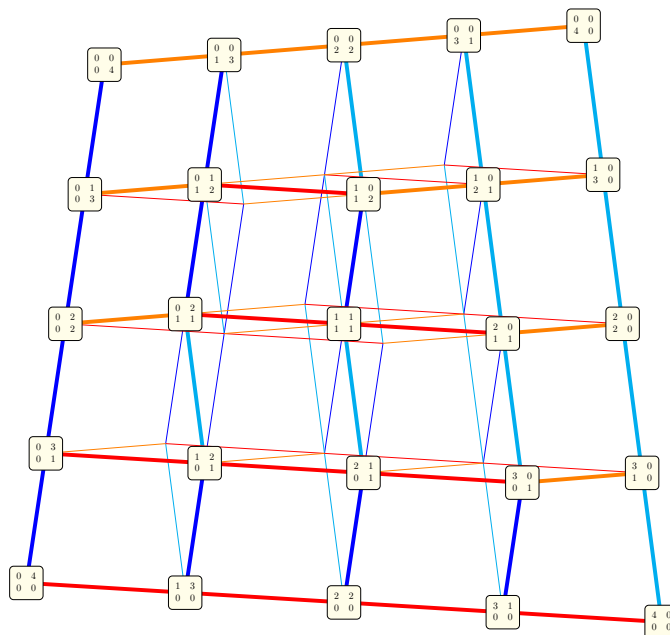


FIGURE 10. The 1-skeleton of the top-dimensional spine from Figure 8 inside the tetrahedral graph of $MULT_4(\mathbf{Q})$.